Neuro-Oncology 12(10):1043–1049, 2010.
doi:10.1093/neuonc/noq056
Advance Access publication May 25, 2010

Influence of blood-brain barrier efflux pumps on the distribution of vincristine in brain and brain tumors

Fan Wang, Feng Zhou, Gary D. Kruh, and James M. Gallo

Department of Pharmacology and Systems Therapeutics, Mount Sinai School of Medicine, New York, New York (F.W., J.M.G.); Department of Pharmacology, Philadelphia, Pennsylvania (F.Z.) and Department of Medicine and Cancer Center, University of Illinois at Chicago, Chicago, Illinois (G.D.K.)

Vincristine (VCR) is efficacious in some but not all brain cancers and an established substrate of Pgp and Mrp1. However, the extent to which such transporters affect the VCR penetration through the blood-brain barrier (BBB) is poorly understood. To evaluate the role of Pgp and Mrp1 in VCR CNS distribution, VCR concentrations were analyzed under steady-state conditions in normal brain, brain tumor, and bone marrow in wild-type (WT), Mrp1 ko (*mrp1*−/−), Pgp ko (*mdr1a*−/−:*mdr1b*−/−), and TKO (*mdr1a*−/−:*mdr1b*−/−:*mrp1*−/−) mice. VCR normal brain partition coefficients (i.e. tissue/plasma VCR concentrations) in TKO mice were greater than those in WT mice at both targeted 10 and 50 ng/mL plasma VCR concentrations, and ranged from 1.3- to 3.6-fold. VCR brain tumor partition coefficients in Mrp1 mice were greater than WT mice at both doses, being 1.5- and 2.4-fold higher at low and high doses, respectively. TKO mice also showed elevated VCR brain tumor penetration with a brain tumor partition coefficient of 1.9-fold greater than that in WT mice at the high-dose level. The bone marrow partition coefficient in Mrp1 ko mice was 1.65-fold greater than that in WT mice. Within strain comparisons revealed that VCR brain tumor concentrations were significantly greater than normal brain in all strains, ranging from 9- to 40-fold. These findings indicate that disruption of the BBB caused the largest enhancement in VCR tumor concentrations, yet the absence of Mrp1 on the brain tumor vasculature could enhance the penetration compared with that in normal brain.

Received February 9, 2010; accepted April 15, 2010.

Corresponding Author: James M. Gallo, Pharm.D., PhD, Department of Pharmacology and System Therapeutics Mount Sinai School of Medicine One Gustave L. Levy Pl Box 1603 New York, NY, 10029 (james.gallo@mssm.edu).

Keywords: brain tumor, partition coefficient, pharmacokinetics, vincristine.

Vincristine (VCR), a plant alkaloid that interferes with microtubule function, is widely employed as an anticancer agent. In addition to its use in hematopoietic malignancies, it is also used in the treatment of different types of brain tumors.[1–3] With respect to brain tumors, VCR is a component of the well-known PCV triple drug regimen, which consists of procarbazine (P), CCNU (C), and VCR. PCV is a chemotherapeutic option for anaplastic oligodendrogliomas, anaplastic oligoastrocytomas, and recurrent brain tumors.[4] The arrival of temozolomide has diminished the use of PCV, and based on the low blood-brain barrier (BBB) transport and disparate clinical trial results, the continued use of VCR in central nervous system (CNS) tumors has been questioned.[5] Nonetheless, for patients with anaplastic oligodendrogliomas and anaplastic oligoastrocytomas that have 1p and 19q chromosomal codeletions, the response rate to PCV is 100%;[6] thus PCV remains an option for certain types of malignant brain tumors.

The entry of VCR into the brain is expected to be low owing to its large size (MW ~825 daltons) and its susceptibility to transport by Mrp1 and Pgp. Specific measurements of the distribution of VCR in the CNS are quite limited in the literature. It has been demonstrated both in pediatric acute lymphoblastic leukemia (ALL) patients and adult non-Hodgkin's lymphoma patients treated at therapeutic doses of VCR that cerebrospinal fluid (CSF) concentrations were no greater than 5% of those in plasma.[7,8] Of course, the distribution of drugs into the CSF are not necessarily representative of drug distribution in brain, and even less so of distribution in brain tumors in which the BBB is compromised and more permissive to drug uptake. A single study using the 9 L intracerebral tumor model in rats and radiolabeled VCR administered intra-arterially concluded that normal brain and brain tumor penetration of

VCR was quite low, in part due to Pgp located at the BBB. However, since plasma concentrations were neglected, the fractional uptake could not be determined and clear inferences on the role of Pgp could not be drawn.[5]

In addition to Pgp and Mrp1, other MRP family members may affect its pharmacokinetics and also contribute to a drug-resistant phenotype in cancer cells.[9–13] Surprisingly, there are few animal studies to examine the role of both Pgp and Mrp1 at the BBB in anticancer drug distribution, which prompt us to perform the current study. To analyze the contribution of Pgp and Mrp1 to VCR distribution, measurements of VCR were made in brain, brain tumors, plasma, and bone marrow, a site of VCR toxicity in mice that lacked Pgp and/or Mrp1 (*mdr1a−/−:mdr1b−/−*, *mrp1−/−* and the triple knockout, *mdr1a−/−:mdr1b−/−:mrp1−/−*) under steady-state drug conditions. By comparing the drug distribution in brain tumor and normal brain, the selective penetration of VCR in tumors could be assessed, and the respective roles of the pumps could be inferred.

Materials and Methods

Chemicals

VCR sulfate was purchased from Hande Tech USA Inc. All other chemicals were purchased from Sigma Chemical Co. The B16 mouse melanoma cell line was kindly provided by Dr Klein-Szanto, Fox Chase Cancer Center. FVB parental, *mrp1−/−*, *mdr1a−/−*: *mdr1b−/−*, and *mdr1a−/−:mdr1b−/−:mrp1−/−* triple knockout mice were provided by Taconic.

In Vivo Intracerebral Tumor Models

A syngeneic tumor model was needed for compatibility with the mouse strains. Since B16 melanoma was readily distinguished from the normal brain due to its darker pigment, it facilitated gross dissection to obtain tumor samples and met the requirement for a syngeneic model. Therefore, we used the B16 melanoma tumor as the in vivo intracerebral tumor model, as we reported previously.[14] Briefly, mice (male, weighing 25–30 g) were anesthetized with an i.p. dose (0.1 mL/10 g body weight) of a 3:2:1 (V:V:V) mixture of ketamine hydrochloride (10 mg/mL):acepromazine maleate (1 mg/mL):xylazine hydrochloride (2 mg/mL), secured in a stereotaxic apparatus, and had implanted 3 μL of a B16 tumor cell suspension (10^8 cells/mL) into the right (2.5 mm lateral from the bregma) thalamic region at a depth of 3 mm. The hole was sealed with bone wax, and the skin was sutured. The mice were then returned to cages and received a standard mouse diet and water ad libitum. Animals were monitored daily for CNS symptoms such as unsteady gait, arched back, unkempt appearance, and body weight. At the first sign of symptoms or a 10% loss in body weight, the animals were entered into the pharmacokinetic (PK) studies. All procedures were conducted in accordance with the NIH Guidelines Concerning the Care and Use of Laboratory Animals and were approved by the Institutional Animal Care and Use Committee.

Pharmacokinetic Studies

The goal of the PK studies was to compare VCR brain, brain tumor, and bone marrow distribution in wild-type (WT), *mrp1*$^{-/-}$ (Mrp1 ko), *mdr1a/b*$^{-/-}$ (Pgp ko), and *mdr1a/b/mrp1*$^{-/-/-}$ (TKO) mice under steady-state conditions.

The progression from tumor cell implantation to exhibiting CNS symptoms and weight loss in each mouse strain was reproducible and occurred at about 10 days following cell implantation. At this time, animals were anesthetized as described above and had implanted both a right carotid artery and jugular vein cannula for blood sampling and dosing, respectively. Systemic PK parameters could differ in different ABC transporter KO mice; thus a preliminary PK study was conducted to obtain CL and V_{ss} values in each strain used in this study. The CL and V_{ss} values were further used to calculate the loading dose and constant infusion rate employed in each strain. To achieve steady-state VCR plasma concentrations of 10 ng/mL, WT mice received a loading dose of 0.19 mg/kg and a constant rate infusion of 0.91 μg/kg/min for 4 h, whereas Mrp1 ko, Pgp ko, and TKO strains received loading doses of 0.37, 0.19, and 0.24 mg/kg, respectively, and a constant rate infusion at 0.97, 0.69, and 0.80 μg/kg/min, respectively. Similarly, to achieve 50 ng/mL VCR plasma steady-state concentrations, corresponding loading doses and infusion rates used for 10 ng/mL steady-state study were proportionally increased by a factor of 5. During the 4 hour VCR infusions, 30 μL blood samples were collected from the right common carotid artery at 60, 120, 180, and 240 minutes. Plasma was harvested from each blood sample and stored at −80°C until analyzed for VCR by liquid chromatography-mass spectrometry (LC-MS) (see below). Immediately after the 240 minutes blood samples were collected, mice were anesthetized with ether and sacrificed by cervical dislocation, and the whole brain was removed and frozen in dry ice before storage at −80°C. For subsequent analysis by LC-MS, partially frozen brains were sectioned into normal brain and brain tumor samples. Normal brain, brain tumor, and bone marrow VCR concentrations measured by LC-MS were used to calculate the corresponding partition coefficients, the ratios of steady-state VCR brain, brain tumor, and bone marrow concentrations to VCR plasma concentrations measured at 240 minutes. Statistical comparisons and VCR partition coefficients were made between strains and between low and high steady-state plasma concentration levels using 2-sided Student's *t*-tests. A value of $P < 0.05$ was considered statistically significant.

Quantitation of VCR by LC-MS

A previously reported LC-MS assay was used to measure the VCR in plasma and tissue samples because it

afforded improved sensitivity with small sample volumes.[15] Plasma samples were thawed to room temperature, and 10 μL aliquots were added to 100 μL of methanol. After a 1 minute vortex and centrifugation (18 000 × g for 3 minutes), the supernatant was collected and added to 20 μL of a 0.17 μM internal standard (vinblastine) solution and 900 μL water, the mixture was then passed through a preconditioned (washed with 1 mL methanol and 2 mL water) solid phase C2 cartridge. The cartridge was then washed with 1 mL of water and 2 mL of 50% methanol in water followed by gradual elution of the desired components with 300 μL of a solution consisting of methanol and 15 mM ammonium acetate (70:30). Forty microliter aliquots of the eluants were injected onto the LC–MS system that consisted of an analytical column (Phenomenex, Luna 3u C8 [2], 3 μm particle size, 50 mm × 2.0 mm) maintained at room temperature and mobile phase of 70% methanol in 15 mM ammonium acetate with 0.1% formic acid (V/V) pumped at a flow rate of 0.2 mL/min. VCR and vinblastine (internal standard) were detected at m/z ratios of 825 and 812, respectively.

To thawed left brain (contralateral hemisphere to the tumor), right brain, and brain tumor samples, 19 times the volume of water was added and homogenized under ice-cold conditions for 10 seconds of which 100 μL of homogenate was mixed with 300 μL of methanol by vortex for 1 minute, and then centrifuged at 18 000 × g for 3 minutes. The resultant supernatant was mixed with 20 μL of the internal standard working solution and 800 μL of water, and then applied to a preconditioned C2 cartridge and processed as for plasma. Bone marrow concentrations of VCR were based on samples collected from femur bones. Briefly, femur bone was fissured and 500 μL of water was added for sonication for 30 minutes. An aliquot of 50 μL of the processed sample was mixed with 150 μL of methanol by vortex for 1 minute and then centrifuged at 18 000 × g for 3 minutes. The resultant supernatant was mixed with 20 μL of the internal standard working solution and 900 μL of water and then applied to a preconditioned C2 cartridge and processed as for plasma. The concentration of VCR was normalized to the weight of the bone sample. The assay for each sample type was both accurate and precise with within and between-day coefficients of variation of <15%.

Results

Preliminary PK Studies

Given that the systemic PK properties of VCR could differ between each strain due to the influence of Pgp and Mrp1 on drug distribution and elimination, single-dose IV bolus administration of 4 mg/kg of VCR was performed in each strain to measure total clearance (CL) and the volume of distribution at steady state (V_{ss}) (Supplementary Material, Table S1). Total clearance was not statistically different between strains and the values ranged from a low of 69.2 mL/min/kg in Pgp knockout mice to 97.4 mL/min/kg in the Mrp1 knockout group. The reduced clearance in the Pgp knockout group is attributed to a lack of Pgp-mediated biliary excretion of VCR. The value of V_{ss} in the Mrp1 ko mice was about 2-fold higher than that in WT mice ($P < 0.05$). Regardless of the differences in the PK parameters between strains, the actual values of CL and V_{ss} were used to design the steady-state dosing regimens. These regimens were administered for 4 hours in each strain through the combined administration of an IV bolus dose and constant rate infusion that would provide equivalent plasma concentrations of VCR in each strain (see Materials and Methods). Two steady-state PK studies of VCR were completed, one that targeted plasma concentrations of 10 ng/mL and another at 50 ng/mL.

Steady-State Plasma Concentrations in WT and ABC Transporter Gene–Disrupted Mice

Plasma concentrations of VCR in WT, Mrp1 ko, Pgp ko, and TKO mice administered 1 of 2 steady-state dosing regimens are illustrated in Fig. 1. The steady-state VCR regimens employed a simultaneous IV bolus and continuous IV infusion for 4 hours, which achieved steady state expeditiously. In the low-dose study, which targeted steady-state plasma concentration of ~10 ng/mL, mean VCR plasma concentrations were essentially constant between 180 and 240 minutes with mean values that ranged from 9 ± 3 to 12 ± 3 ng/mL, which were not significantly different between strains (Fig. 1). Similarly, in the high-dose study targeting VCR plasma concentrations of ~50 ng/mL, mean

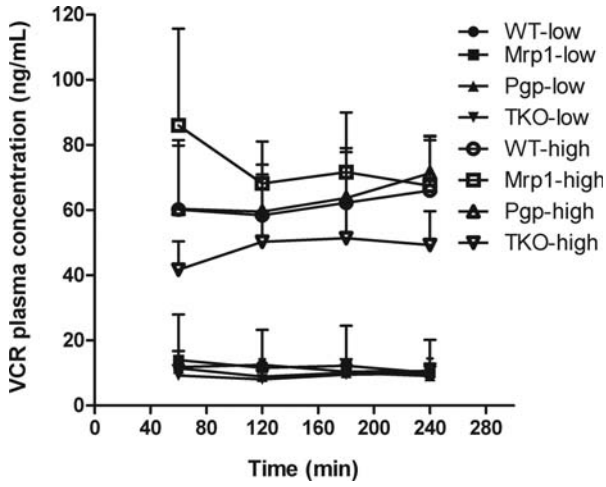

Fig. 1. Mean (± SD) VCR plasma concentrations at 60, 120, 180, and 240 minutes. VCR was administered as a combined IV bolus dose and a 4 hour IV infusion designed to achieve plasma concentrations of 10 ng/mL (low dose, $n = 6$, filled symbols) and 50 ng/mL (high dose, $n = 10$, open symbols), respectively. Between 180 and 240 minutes, VCR plasma concentration reached steady state in both low- and high-dose study. WT (circle); Mrp1 ko (square); Pgp ko (triangle); TKO (inverted triangle).

VCR plasma concentrations were constant between 180 and 240 minutes in all groups. This confirmed the achievement of steady state in both the low- and high-dose groups. It is worth noting that in the high-dose study, VCR steady-state plasma concentrations in TKO mice were significantly lower, being 49.3 ± 10.4 ng/mL, than those in the other strains, which were 66.0 ± 15.5 ng/mL in the WT group, 71.4 ± 11.3 ng/mL in the Pgp ko group, and 67.5 ± 15.3 ng/mL in the Mrp1 ko group (Fig. 1).

There were minimal differences in normal brain VCR concentrations across strain and dose levels with only TKO mice possessing higher left brain ($P < 0.01$) and right brain ($P < 0.05$) VCR concentrations than those in WT mice in low-dose study. Finally, bone marrow VCR steady-state concentrations in Mrp1 ko mice (Table 1, $P < 0.01$) were significantly higher than that in WT mice at the high dose, the only dose studied, whereas no differences were found in other knockout animals.

VCR Tissue Concentrations in WT and ABC Transporter Gene–Disrupted Mice

VCR concentrations were compared both within strains and between strains. Comparisons of VCR concentrations within each strain indicated that VCR brain tumor concentrations were statistically greater ($P < 0.0001$) than either the left or the right brain, ranging from ~11- to 40-fold higher at the low-dose level or from ~9- to 28-fold higher at the high-dose level (Fig. 2B) (Table 1). As expected, left and right brain VCR concentrations within each strain did not differ from each other ($P > 0.05$).

Comparisons of brain tumor VCR concentrations between ABC transporter knockout and WT animals revealed differences in both the low- and high-dose studies. In the low-dose study, tumor concentration in Mrp1 ko mice (60.4 ± 15.9 ng/g) was ~1.5-fold greater ($P < 0.05$) than that in WT mice (40.4 ± 15.9 ng/g), whereas no differences of tumor concentrations were detected in the other knockout strains compared with WT mice. In the high-dose study, as shown in Table 1, all 3 ABC transporter gene–disrupted strains showed higher tumor concentrations than those in WT mice.

VCR Partition Coefficients in WT and ABC Transporter Gene–Disrupted Mice

Although equivalent steady-state VCR plasma concentrations enable direct comparisons of brain concentrations, analysis of partition coefficients, calculated as the tissue-to-plasma steady-state concentration ratios, provides the most accurate assessment of drug distribution because plasma concentrations, even under steady-state conditions, are not equal in each strain. Plasma drug concentrations are an important factor driving drug penetration into tissues and any differences in plasma concentrations are accounted for in the tissue-to-plasma ratios. The pattern of partition coefficient values with respect to both brain region and genetic type is similar to the pattern observed for VCR brain and brain tumor concentrations.

The mean (± SD) partition coefficients for each brain region and strain for the low-dose (targeted 10 ng/mL plasma VCR) and high-dose (targeted 50 ng/mL plasma VCR) groups are shown in Fig. 2A and B, respectively. Specifically, in the low-dose groups, the VCR tumor partition coefficient in Mrp1 ko mice was ~1.56-fold higher than that in WT mice ($P < 0.05$). In addition, consistent with the normal brain concentration

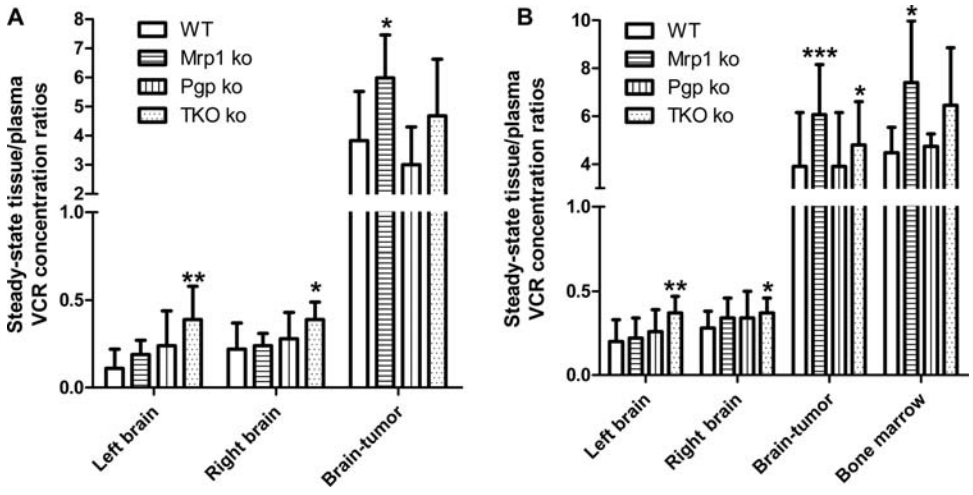

Fig. 2. Steady-state VCR concentration ratios in tissues of wild-type and knock out mouse strains. (A) Low-dose study targeting ~10 ng/mL; (B) high-dose study targeting ~50 ng/mL. For the low-dose group, concentration ratios are shown for left brain, right brain, and brain tumor; for the high-dose group, concentration ratios are shown for left brain, right brain, brain tumor, and bone marrow. WT (open bar); Mrp 1 ko (horizontal stripes); Pgp ko (vertical stripes); TKO (dots). Mean (± SD) are shown; the data are from Table 1. *$P < 0.05$; **$P < 0.01$; ***$P < 0.001$ compared with WT using student's *t*-test.

Table 1. Steady-state tissue VCR concentrations (mean ± SD) in plasma, normal brain, brain tumors, and bone marrows in B16 melanoma-bearing mice following a combined IV bolus dose and a 4 hour IV infusion targeting 10 and 50 ng/mL VCR plasma concentration in WT mice and 3 different ABC transporter gene–disrupted mice

Parameters	WT		Mrp1 ko		Pgp ko		TKO	
	10 ng/mL	50 ng/mL	10 ng/mL	50 ng/mL	10 ng/mL	50 ng/mL	10 ng/mL	50 ng/mL
ss C_p (ng/mL)	10.7 ± 3.8	66.0 ± 15.5	10.1 ± 1.2	67.5 ± 15.3	9.1 ± 3.0	71.4 ± 11.3	9.9 ± 3.0	49.3 ± 10.4*
ss C_{br} (l) (ng/mL)	1.1 ± 0.9	12.9 ± 9.4	2.0 ± 0.9	15.3 ± 8.7	2.0 ± 1.4	17.7 ± 8.5	3.6 ± 1.2**	17.7 ± 4.2
ss C_{br} (r) (ng/mL)	2.2 ± 1.3	17.7 ± 6.4	2.4 ± 0.8	23.2 ± 9.4	2.4 ± 1.1	23.7 ± 10.4	3.7 ± 0.5*	17.4 ± 3.6
ss C_t (ng/mL)	40.4 ± 15.9	163.3 ± 60.7	60.4 ± 15.9*	413.8 ± 202.0**	26.1 ± 10.4	264.8 ± 104.4*	43.7 ± 13.8	228.5 ± 76.6*
ss C_{bm} (ng/g bone)		309.5 ± 40.9		489.2 ± 125.7**		346.5 ± 54.8		298.9 ± 41.3

ss C_p, steady-state VCR plasma concentration; ss C_{br} (l), steady-state VCR left normal brain concentration; ss C_{br} (r), steady-state VCR right normal brain concentration; ss C_t, steady-state VCR tumor concentration; ss C_{bm}, steady-state VCR bone marrow concentration.
*$P < 0.05$; **$P < 0.01$ compared with WT group using student's *t*-test.

data, VCR left and right brain partition coefficients in TKO mice were also significantly higher than those in WT mice at both dose levels. In the high-dose groups, as shown in Fig. 2B, VCR tumor partition coefficients in Mrp1 ko and TKO mice, but not Pgp ko mice, were 2.35- and 1.86-fold greater than those in WT mice ($P < 0.001$ and $P < 0.05$, respectively). In Fig. 2B, the bone marrow VCR partition coefficient in Mrp1 ko mice (7.41 ± 2.57, $P < 0.05$) was significantly higher than that in WT mice (4.48 ± 1.06), whereas no differences were found in other knockout animals.

Discussion

Although VCR PK has been studied extensively and across species,[16] little has been collected on its direct CNS distribution, and to our knowledge this is the first study to address the role of Mrp1 and Pgp at the BBB on its CNS distribution. Through our analysis we can infer that pump inhibitors of Mrp1 can favorably enhance brain tumor distribution of VCR. The other major finding is that disruption of the BBB by the tumor caused a dramatic increase in VCR tumor penetration compared with normal brain.

The function of membrane transporters as determinants of the PK properties of drugs has been avidly documented in both preclinical and clinical investigations.[17,18] These transporters, such as the ABC pumps studied here, may alter drug concentrations in any compartment separated by a membrane in which the pumps operate. The compartment-specific alterations in drug concentrations could manifest as alterations in the systemic PK properties, such as drug clearance and the volume of distribution, as well as localized perturbations in tissues of interest. The current study considered both the systemic and regional effects of 2 ABC pumps, Mrp1 and Pgp, on the disposition of VCR. First, since VCR's systemic PK properties can be impacted by Pgp's action to eliminate it into bile and urine and Mrp1's action to limit tissue distribution due to its basolateral membrane location, single-dose IV VCR studies were completed in each mouse strain to accurately assess the systemic PK properties of VCR in each strain. These parameters (see Supplementary Material, Table S1) indicated both Pgp and Mrp1 influenced the clearance and volume of distribution of VCR and further provided the basis to design steady-state regimens of VCR to target either 10 or 50 ng/mL plasma concentrations. All strains achieved nearly equivalent VCR plasma steady-state concentrations in the low-dose studies, whereas in the high-dose group there was a disparity between the TKO group and the other 3 strains and led to plasma concentrations that ranged from about 50 ng/mL in the TKO group to between 66 and 71 ng/mL in the other 3 strains. There is no obvious explanation for these differences, since even if the assumption of linear kinetics applied to the design of the steady-state dosing protocols was violated in the pilot IV dosing studies, it would unlikely be the case that the much lower plasma concentrations were achieved in the steady-state studies. Finally, it should be appreciated that steady-state conditions were achieved at about 2 hours in all groups, and thus, time-dependent changes in VCR's tissue distribution were negated. There are 2 key comparisons that can be made from the steady-state experiments: (i) the inter-strain changes in tissue/plasma ratios and (ii) intra-strain differences between brain tumor and normal brain VCR concentrations. The inter-strain comparisons in VCR's tissue distribution (Fig. 2) revealed the most profound differences in normal brain occurred in the TKO strain, being in the range of 1.3–3.7-fold greater at both targeted plasma concentrations. Singular deletions of either Pgp or Mrp1 at the BBB did not significantly modulate VCR's ability to penetrate the BBB as each can apparently compensate for one another and limit VCR's uptake in normal brain. The inability of singular deletions of Pgp at the BBB to enhance VCR brain uptake is not unexpected even though paclitaxel in an analogous experimental model of the Pgp knockout showed significant, approximately 2-fold increases in normal brain penetration.[14] The differential finding between VCR and paclitaxel attests to the fact that paclitaxel is not a substrate for

Mrp1, as VCR or other BBB efflux pumps that might perform a compensatory function. The compensatory efflux function afforded by Mrp1 at the BBB supports its high capacity and apical location. With regard to the latter, some studies have shown that Mrp1 is located on the basolateral side of the membrane outside the BBB,[19] whereas another indicated an apical localization of Mrp1 at the BBB,[20,21] which now seems more plausible based on the current results. Therefore, attenuation of both Mrp1 and Pgp seem necessary to appreciably enhance the VCR uptake in normal brain.

The pattern of VCR distribution in brain tumors among the 4 strains is somewhat altered compared with that in normal brain with the Mrp1 knockout group, achieving the highest brain tumor/plasma ratios at both targeted steady-state concentrations (Fig. 2). The greater partition coefficient of VCR in the Mrp1 group could reflect a more compromised BBB than in the other strains and would have to be of such a magnitude to offset the negated compensatory effects of the pumps in the TKO group. Even though the time the PK studies are conducted following tumor cell implantation are relatively constant, being about 10 days after implantation, there is heterogeneity, as reflected in the standard deviations (Fig. 2 and Table 1), which may reflect variations in the integrity of the BBB. This variability could lead to, on average, a more disrupted BBB in the Mrp1 knockout group that would enable VCR's passage into tumor between adjacent endothelial cells and overcome the efflux action of Pgp on the BBB. Thus, a major conclusion that can be drawn from this study is that the absence of Mrp1 at the BBB had the most profound effect among the 4 strains on VCR tumor penetration, being an approximate 1.6–2.4-fold greater than WT mice.

Intra-strain comparisons of VCR distribution between normal brain and brain tumors were fairly consistent with significantly greater VCR tumor concentrations (Table 1), being achieved relative to normal brain, and ranged from ~9- to 40-fold. These findings are not unexpected and are consistent with the disrupted and "leaky" nature of the BBB in brain tumors. Of course this global assessment based on whole tumor homogenates does not reflect regional variations in BBB integrity often associated with the advancing outer rim of the tumor that may have a more normal BBB. In addition, the lumped whole tumor measurements of VCR cannot be used to assess compartment-specific changes in either interstitial fluid or intracellular drug concentrations due to transporters functioning as drug efflux pumps at the level of the tumor cell membrane. Since only one tumor model was used in this investigation, the potential effects of tumor cell drug efflux would be analogous in all strains. The action of drug efflux pumps in tumor cells can be addressed by placing microdialysis probes in the interstitial fluid space of tumors and sampling drug concentrations.[22,23] This strategy was not implemented here due to the poor diffusivity of large MW lipophilic compounds through dialysis membranes. More intricate experimental protocols will likely be required to further delineate VCR compartment-specific distribution and the role of efflux pumps in tumor cells. One approach that is forthcoming from the steady-state design used here would be to compare VCR distribution in transporter-null and over-expressed tumor models to facilitate detection of compartment-specific changes in drug distribution. Overall, VCR distribution into brain tumors was significantly elevated compared with normal brain with the most critical factor being the breakdown of the BBB as opposed to the absence of either Mrp1 or Pgp.

Although VCR causes a variety of CNS toxicities, such as peripheral neuropathy, myelotoxicity is not uncommon, and is a tissue in which ABC transporters could govern drug entry. Since Pgp expression was found in hematopoietic progenitor cells,[24] in vitro and in vivo experiments using ABC transporter knockout animals suggested Pgp and Mrp1 play a role in protecting bone marrow from the VCR toxicity.[25,26] However, without direct assessment of VCR distribution in these ABC transporter knockout animals, a causative relationship between the VCR penetration and toxicity cannot be established. In our experiment, VCR bone marrow tissue concentrations as well as the VCR bone marrow partition coefficients were determined under a steady-state dosing regimen in which the Mrp1 group showed the highest VCR concentrations and partition coefficient and were significantly greater than those compared with the WT group. In contrast, the Pgp group did not differ from the WT group, suggesting a dominant role of Mrp1 in bone marrow protection. In support of this finding, chimera WT mice transplanted with bone marrow from either Mrp1 ko or TKO mice had greater bone marrow toxicity than the chimera WT mice transplanted with WT or Pgp knockout mice donor bone marrow.[25]

A question raised by this investigation is whether modulation of VCR transport by an Mrp1 and/or Pgp transport inhibitor is justified. Clearly, the largest changes in the VCR penetration across all strains is afforded by the disruption of the BBB due to the tumor and if this change occurs throughout the tumor, not a likely phenomenon, further manipulation of drug efflux pumps at the BBB by a transport inhibitor may not be required. However, about 2-fold enhancements might be achievable in brain tumors due to inhibition of Mrp1 or the combination of inhibition of Mrp1 and Pgp, and if regions of the tumor possess an intact BBB, the use of inhibitors could be further justified. These potential advantages could be counteracted by increases in the VCR distribution both in normal brain as well as in the bone marrow that may similarly be affected by the systemic actions of transport inhibitors. An important and possibly deciding factor on the use of a transport inhibitor in conjunction with VCR in brain tumor patients is whether efflux pumps can mediate VCR entry into tumor cells. Further preclinical studies may be warranted to develop strategies to delineate the compartment-specific VCR distribution as mentioned above. In summary, the key findings were that Pgp and Mrp1 can influence the VCR CNS penetration, yet their effects in brain tumors are less than disruption of the BBB due to the tumor itself. Future investigations on the use of transport modulators as a means to increase

VCR tumor concentrations should consider the function of pertinent transporters on the tumor cell membrane as well as regional variations in BBB permeability.

Supplementary Material

Supplementary Material is available at *Neuro-Oncology* online.

Conflict of interest Statement. None declared.

Funding

This study was partially supported by National Institutes of Health grant CA73728.

References

1. Gidding CE, Kellie SJ, Kamps WA, et al. Vincristine revisited. *Crit Rev Oncol Hematol*. 1999;29:267–287.
2. Comis RL. Clinical trials of cyclophosphamide, etoposide, and vincristine in the treatment of small-cell lung cancer. *Semin Oncol*. 1986;13:40–44.
3. Finkel HE. Vincristine therapy. *N Y State J Med*. 1967;67:2474–2478.
4. Wen PY, Kesari S. Malignant gliomas in adults. *N Engl J Med*. 2008;359:492–507.
5. Boyle FM, Eller SL, Grossman SA. Penetration of intra-arterially administered vincristine in experimental brain tumor. *Neuro Oncol*. 2004;6:300–305.
6. Cairncross JG, Ueki K, Zlatescu MC, et al. Specific genetic predictors of chemotherapeutic response and survival in patients with anaplastic oligodendrogliomas. *J Natl Cancer Inst*. 1998;90:1473–1479.
7. Jackson DV, Jr, Sethi VS, Spurr CL, et al. Pharmacokinetics of vincristine in the cerebrospinal fluid of humans. *Cancer Res*. 1981;41:1466–1468.
8. Kellie SJ, Barbaric D, Koopmans P, et al. Cerebrospinal fluid concentrations of vincristine after bolus intravenous dosing: a surrogate marker of brain penetration. *Cancer*. 2002;94:1815–1820.
9. Benyahia B, Huguet S, Decleves X, et al. Multidrug resistance-associated protein MRP1 expression in human gliomas: chemosensitization to vincristine and etoposide by indomethacin in human glioma cell lines overexpressing MRP1. *J Neurooncol*. 2004;66:65–70.
10. Loe DW, Deeley RG, Cole SP. Characterization of vincristine transport by the M(r) 190,000 multidrug resistance protein (MRP): evidence for cotransport with reduced glutathione. *Cancer Res*. 1998;58:5130–5136.
11. Huang R, Murry DJ, Kolwankar D, et al. Vincristine transcriptional regulation of efflux drug transporters in carcinoma cell lines. *Biochem Pharmacol*. 2006;71:1695–1704.
12. Watanabe T, Suzuki H, Sawada Y, et al. Induction of hepatic P-glycoprotein enhances biliary excretion of vincristine in rats. *J Hepatol*. 1995;23:440–448.
13. Stefankova Z, Barancik M, Breier A. Overcoming of P-glycoprotein mediated vincristine resistance of L1210/VCR mouse leukemic cells could be induced by pentoxifyline but not by theophylline and caffeine. *Neoplasma*. 1996;43:11–15.
14. Gallo JM, Li S, Guo P, et al. The effect of P-glycoprotein on paclitaxel brain and brain tumor distribution in mice. *Cancer Res*. 2003;63:5114–5117.
15. Guo P, Wang X, Zhou F, et al. Determination of vincristine in mouse plasma and brain tissues by liquid chromatography-electrospray mass spectrometry. *J Chromatogr B Analyt Technol Biomed Life Sci*. 2004;809:273–278.
16. El Dareer SM, White VM, Chen FP, et al. Distribution and metabolism of vincristine in mice, rats, dogs, and monkeys. *Cancer Treat Rep*. 1977;61:1269–1277.
17. Schinkel AH, Smit JJ, van Tellingen O, et al. Disruption of the mouse mdr1a P-glycoprotein gene leads to a deficiency in the blood-brain barrier and to increased sensitivity to drugs. *Cell*. 1994;77:491–502.
18. Dantzig AH, de Alwis DP, Burgess M. Considerations in the design and development of transport inhibitors as adjuncts to drug therapy. *Adv Drug Deliv Rev*. 2003;55:133–150.
19. Roberts LM, Black DS, Raman C, et al. Subcellular localization of transporters along the rat blood-brain barrier and blood-cerebral-spinal fluid barrier by in vivo biotinylation. *Neuroscience*. 2008;155:423–438.
20. Sugiyama D, Kusuhara H, Lee YJ, et al. Involvement of multidrug resistance associated protein 1 (Mrp1) in the efflux transport of 17beta estradiol-D-17beta-glucuronide (E217betaG) across the blood-brain barrier. *Pharm Res*. 2003;20:1394–1400.
21. Zhang Y, Schuetz JD, Elmquist WF, et al. Plasma membrane localization of multidrug resistance-associated protein homologs in brain capillary endothelial cells. *J Pharmacol Exp Ther*. 2004;311:449–455.
22. Zhou Q, Gallo JM. In vivo microdialysis for PK and PD studies of anticancer drugs. *AAPS J*. 2005;7:E659–E667.
23. Benjamin RK, Hochberg FH, Fox E, et al. Review of microdialysis in brain tumors, from concept to application: first annual Carolyn Frye-Halloran symposium. *Neuro Oncol*. 2004;6:65–74.
24. Chaudhary PM, Roninson IB. Expression and activity of P-glycoprotein, a multidrug efflux pump, in human hematopoietic stem cells. *Cell*. 1991;66:85–94.
25. van Tellingen O, Buckle T, Jonker JW, et al. P-glycoprotein and Mrp1 collectively protect the bone marrow from vincristine-induced toxicity in vivo. *Br J Cancer*. 2003;89:1776–1782.
26. Johnson DR, Finch RA, Lin ZP, et al. The pharmacological phenotype of combined multidrug-resistance mdr1a/1b- and mrp1-deficient mice. *Cancer Res*. 2001;61:1469–1476.